Bioimaging

DOI: 10.1002/smll.200800080

3C–SiC Nanocrystals as Fluorescent Biological Labels**

Jiyang Fan, Hongxia Li, Jiang Jiang, Leo K. Y. So, Yun Wah Lam, and Paul K. Chu**

Quantum dots are superior to dye molecules in many aspects from size-tunable fluorescence and resistance to photobleaching and they have thus been widely used in biology as fluorescent probes.[1,2] However, the cytotoxicity of some quantum dots limits their use in biological systems,[3,4] and exploiting green nanoparticles with low cytotoxicity has become one major concern in this field.[5–8] Silicon carbide, one well-known power electronic semiconductor material, is considered one of the best biocompatible materials, especially to blood.[9] In addition, it has superior properties such as low density, high hardness, high strength, and chemical inertness. In recent years, much effort has been made to synthesize nanocrystalline SiC and study its photoluminescence (PL) properties.[10–16] Some synthesized SiC nanostructures showed emission in the blue-to-UV range with their properties depending sensitively on the fabrication method and even on specific experiments. Although some variations have been reported, in general the observed emissions can be ascribed to some surface or defect states in the SiC nanostructures. However, owing to their relatively large size, low emission intensity, lack of controlled synthesis, and variable optical properties, these interconnected SiC nanostructures can hardly be used as fluorescent biological labels. Kassiba and co-workers synthesized SiC nanoparticles with diameters of tens of nanometers as well as the corresponding nanocomposites by a laser pyrolysis procedure and extensively investigated their optical properties.[17–19] Indeed, one recent paper reported highly fluorescent, ultrasmall colloidal 3C–SiC nanoparticles with diameters of between 1-7 nm.[20,21] Similar emissions have been observed from suspended 6H–SiC nanoparticles.[22] In this Communication, we report for the first time the use of 3C–SiC nanocrystals as biological labels in cell imaging. We analyzed the fluorescence dynamics and surface chemistry of the nanoparticles, which are crucial to their biological use, in order to fathom the electronic and optical properties of SiC crystallites with sizes down to a few nanometers. The nanocrystals are nontoxic and highly resistant against photobleaching. Our results suggest that 3C–SiC nanocrystals are suitable fluorescent biological probes.3C–SiC nanocrystals were prepared by dispersing electrochemically etched n-type polycrystalline 3C–SiC ($N_d = 5 \times 0^{16}\,cm^{-3}$) into an aqueous (pure water) solution.[21] The size of the particles has an approximately normal distribution with the most probable diameter being 3.9 ± 1.1 nm (Figure 1 and 2). Insight into the photophysical properties of 3C–SiC nanoparticles involving their application potential in bioimaging was obtained by analyzing the UV/Vis and time-resolved PL spectra, as shown in Figure 3. The nanoparticles show a monotonically increasing UV/Vis spectrum with an onset at around 2.8 eV (Figure 3a), which is blue shifted with respect to the bandgap of bulk 3C–SiC (2.2 eV, as indicated in Figure 3a), as expected from quantum-confinement effects. The long absorption tail on the lower-energy side reflects the indirect nature of the bandgap.[23] The sharper rise in absorption with increasing photon energies, starting from ≈5.3 eV, may be associated with a second indirect transition because it is lower in energy than the direct bandgap of bulk 3C–SiC. Figure 3b shows the time-resolved PL decay from fluorescent 3C–SiC nanocrystals (the inset displays the corresponding PL spectrum). The PL decay can be satisfactorily fitted by two exponentials: a fast component with $\tau \approx 4.3$ ns (84%) and a slow component with $\tau \approx 10.9$ ns (16%). The latter is substantially longer than that of most commonly used dye molecules and cellular autofluorescence and can be used to separate the nanoparticle emissions from the background signals using various time-gating methods. These double recombination channels may be associated with the two absorption edges, as revealed by the absorption spectra. We measured the quantum yield of the 3C–SiC nanocrystal solution using quinine sulfate[24] in 0.1 N sulfuric acid as a standard with 360-nm excitation. The quantum yield achieved was 17%, which was greater than those of traditional silicon nanocrystals[25] and comparable to some II–VI-group semiconductor quantum dots[26] as well as some dye molecules. To the best of our knowledge, this is the first quantitative identification of quantum efficiency in SiC nanocrystals. Our results reveal that fluorescence is largely enhanced in nanocrystalline SiC compared to bulk SiC (an indirect bandgap semiconductor with poor emission) because of significant suppression of the nonradiative processes in the nanoparticles.[27]

Previous work has shown that the surface features on SiC can influence the solubility of SiC nanocrystals and their reactivity to ambient surrounding media.[18,19] Their electronic

[*] Dr. J. Y. Fan
Department of Physics
Southeast University
Nanjing 211189 (P.R. China)
and Department of Physics and Materials Science
City University of Hong Kong
Kowloon, Hong Kong (P.R. China)
E-mail: jyfan@seu.edu.cn
Dr. H. X. Li
Department of Applied Physics
Nanjing University of Science and Technology
Nanjing 210094 (P.R. China)
Dr. J. Jiang, Prof. Paul K. Chu
Department of Physics and Materials Science
City University of Hong Kong
Kowloon, Hong Kong (P.R. China)
E-mail: paul.chu@cityu.edu.hk
Dr. L. K. Y. So, Dr. Y. W. Lam
Department of Biology and Chemistry
City University of Hong Kong
Kowloon, Hong Kong (P.R. China)

[**] We thank K.K.W. Low and Y. Zhang for their assistance with some of the characterization work. This work is supported by grants from the Hong Kong Research Grants Council (RGC) under Competitive Earmarked Research Grants (CERG) Nos. CityU 112306 and CityU 112307.

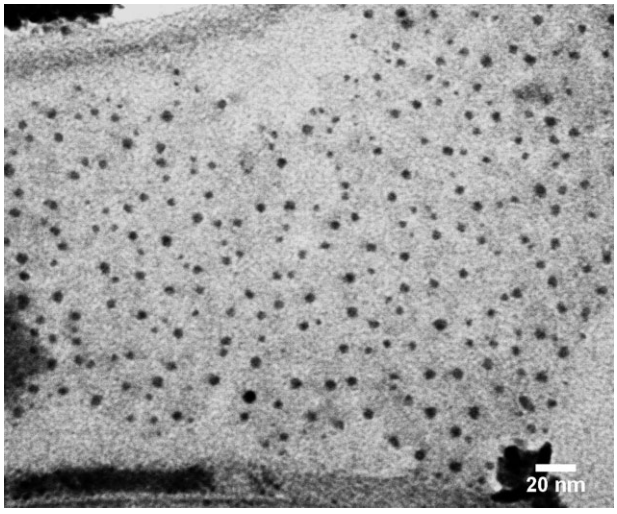

Figure 1. Transmission electron microscopy (TEM) image of 3C–SiC nanocrystals obtained by dipping several drops of 3C–SiC nanocrystal solution onto the graphite grid.

structure and emission properties[22,28,29] thus need to be clarified in order to understand the effects of aqueous solvents and their interaction with 3C–SiC nanocrystals. Figure 4 shows the infrared transmission spectrum of the 3C–SiC nanocrystal solution in optically clear KBr pellets measured after evaporation of water. The strong absorption bands associated with water cannot be observed due to evaporation. All the peaks displayed in Figure 4 show no obvious decrease in the intensity after water evaporation and should therefore be associated with 3C–SiC nanocrystals, as reported previously.[13,30] The Si–C stretching mode is seen at 700–850 cm^{-1} with a frequency downshift with respect to the bulk SiC material and it may be induced by phonon confinement in the quantum dots.[31] The peak at 482 cm^{-1} originates from Si–$(OH)_n$ bonds. The features at 1084 and 1124 cm^{-1} may be assigned to C–N or C–O–Si stretching modes. Our results are in agreement with former reports that water molecules can easily dissociate at Si-terminated SiC surfaces at room temperature,[32–34] forming Si–OH bonds and leading to the

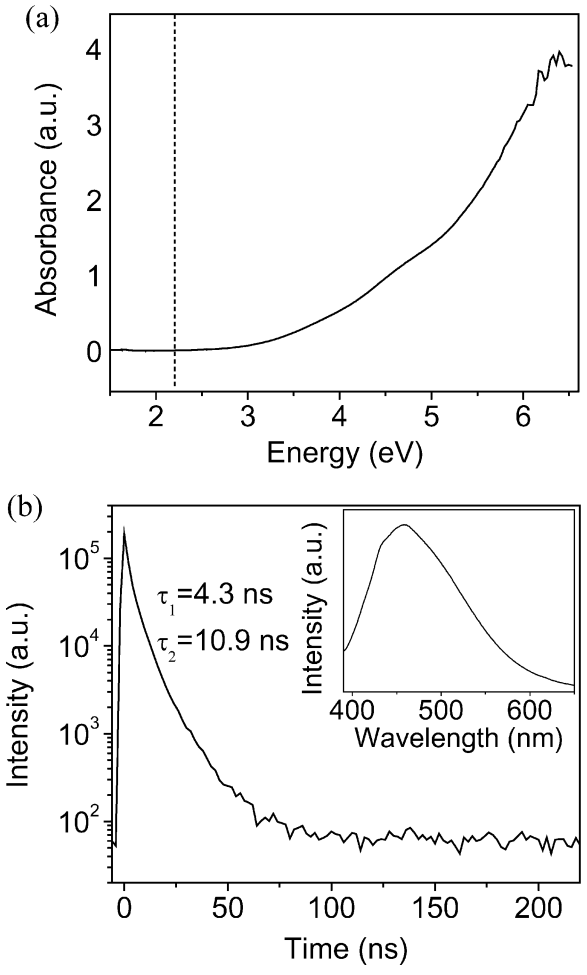

Figure 3. a) Room temperature UV/Vis absorbance spectrum of 3C–SiC nanocrystals dispersed in pure water. The dotted line indicates the position of bandgap of bulk 3C–SiC. b) Time-resolved PL decays monitored at 454 nm with an excitation wavelength of 375 nm for the same sample, which can be well fitted by using two exponentials with lifetimes as indicated. The inset is the corresponding emission spectrum excited at 375 nm.

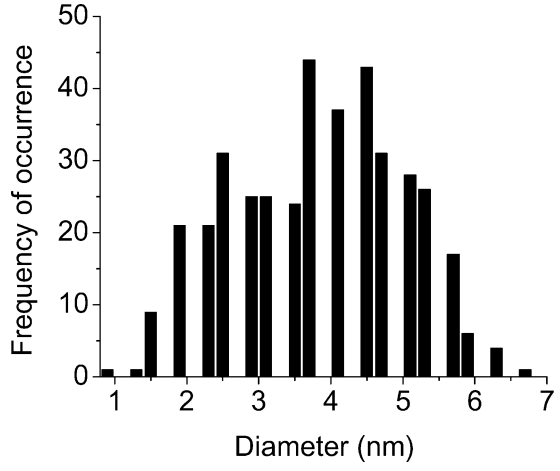

Figure 2. Size distribution of 3C–SiC nanocrystals counted for over 400 particles. A Gaussian fit gives a most probable diameter of 3.9 ± 1.1 nm.

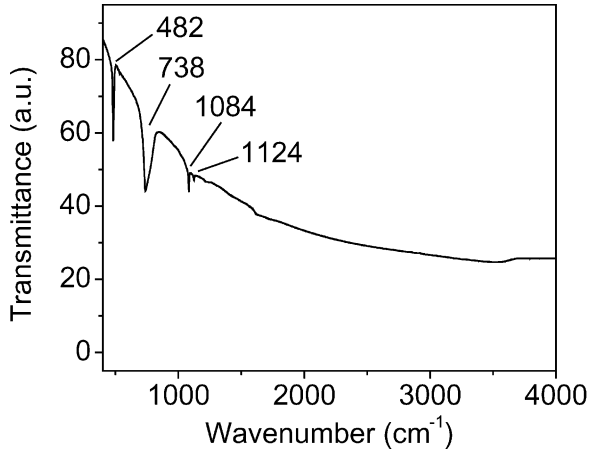

Figure 4. Infrared transmission spectrum of 3C–SiC nanocrystal in a KBr pellet.

saturation of the dangling bonds. Surface passivation induced by the surrounding media excludes potential surface states so that the occurrence of interband transitions and corresponding emissions are assured. Molecular dissociation on the surface of the 3C–SiC nanoparticles also explains their good solubility in pure water. Surprisingly, all the distinctive features in the infrared spectra obtained from the 3C–SiC nanocrystal solution are still there after the samples have been left out in air for over two months. The observation discloses the ultrastability of the surface composition of suspended 3C–SiC nanocrystals. It also explains our observation that small 3C–SiC nanoparticles can remain well dispersed in an aqueous solution, retaining the PL intensity for several months. In contrast, traditional II–VI-group quantum dots are mostly synthesized in nonpolar organic solvents and different strategies are needed for stabilization in aqueous buffer.[1]

The water-soluble, inert, and highly luminescent 3C–SiC nanocrystals can be used as biological labels. Human fetal osteoblast (hFOB) cells[35] were used in our 3C–SiC nanocrystal-uptake experiments. After the uptake, the 3C–SiC nanocrystal-labeled hFOB cells show bright fluorescence (Figure 5). Observation of intracellular green–yellow spots implies that the 3C–SiC nanocrystals may penetrate the cell membrane by endocytosis.[36] The cellular autofluorescence is negligible as it is rather weak and its intensity drops quickly with time. Fluorescence is observed throughout the cells, including cell nuclei, suggesting the presence of the nanocrystals in the nuclei. This is consistent with the small size of nanocrystals that should allow their free diffusion through the nuclear pores. This result implies that the small dimension of 3C–SiC quantum dots is a merit and may render them ideal in the imaging of various biological systems at the molecular level. The photostability of 3C–SiC nanocrystals in biological imaging is compared to that of organic dye propidium iodide (PI). Figure 6a depicts the quantitative changes in the fluorescence intensity of the hFOB cells imaged with 3C–SiC nanocrystals and PI, respectively. The fluorescence from the PI-labeled cells diminishes to half of the original intensity in 5 min. In contrast, the fluorescence from the 3C–SiC nanocrystal-labeled cells drops only slightly in the first few minutes upon excitation, after which the fluorescence intensity is maintained for up to 40 min. This resistance to photobleaching is comparable to conventional quantum dots that are photostable for minutes to hours.[1,26]

To quantitatively evaluate the toxicity or biocompatibility of 3C–SiC nanocrystals, methyl thiazolyl tetrazolium (MTT) assay was conducted on a human cervical carcinoma cell line HeLa. The MTT assay is a colorimetric test that assesses the mitochondrial function (a crucial role in maintaining cellular structure and function via aerobic adenosine triphosphate (ATP) production)[37] of cultured cells and is routinely used for the estimation of cell numbers. Cells treated with 3C–SiC nanocrystals at concentrations of up to 100 μg mL^{-1} (or $\approx 1.0 \times 10^{15}$ particles) for as long as 48 h showed no significant difference in the MTT colorimetric reaction compared to controlled cells grown in the absence of nanocrystals for the same length of time (Figure 6b). Phase-contrast microscopy also failed to detect any changes in the cell morphology or any increase in the incidence of dead cells, even in cells treated

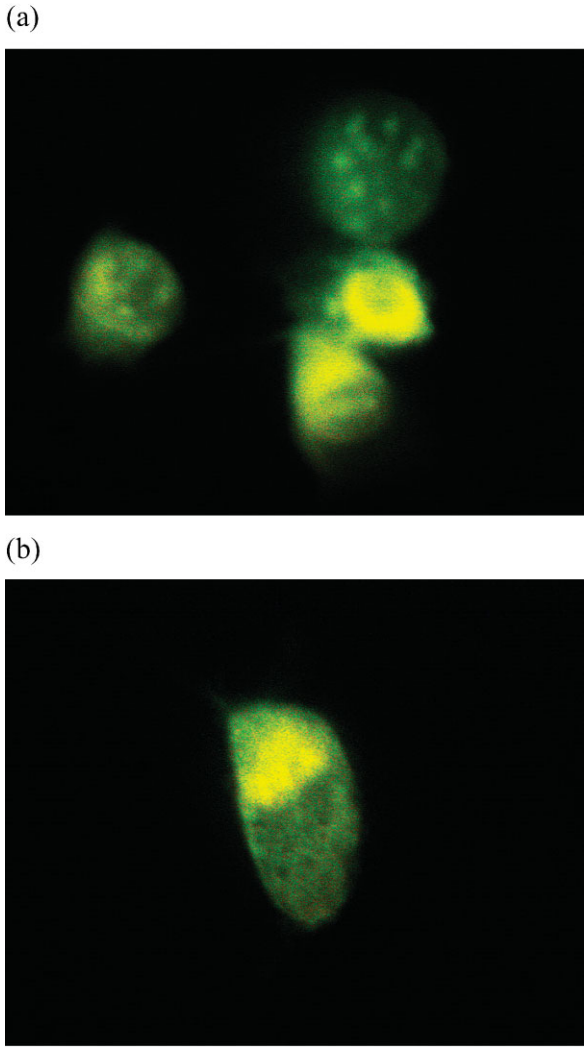

Figure 5. a, b) Images of hFOB cells after 3C–SiC nanocrystal uptake excited at 420–490 nm and examined with a fluorescence microscope. Image width: 93 μm.

with the highest dose of nanocrystals (100 μg ml^{-1}) for the longest time (48 h; data not shown). The results suggest that even at high concentration and continuous exposure for two days the 3C–SiC nanocrystals exhibit no detectable toxicity and no inhibitory effect on cell proliferation. This is consistent with our expectation since silicon carbide has excellent chemical inertness and no toxic ions are released.

In summary, we have demonstrated that 3C–SiC quantum dots prepared by simple electrochemical etching together with ultrasonic stirring can be introduced into cells and serve as robust nontoxic biological probes with low photobleaching and long-term stability. We are currently conducting more experiments to attain SiC surface functionalization and to link the functionalized nanocrystals to various biological ligands such as proteins and antibodies for probing and imaging. The co-existence of the H-terminated hydrophilic surface and C-terminated hydrophobic surface in 3C–SiC dots makes them favorable to functionalization with different types of biomolecules.[38] Another merit of 3C–SiC nanocrystals as biological labels is their tunable emissions across the whole

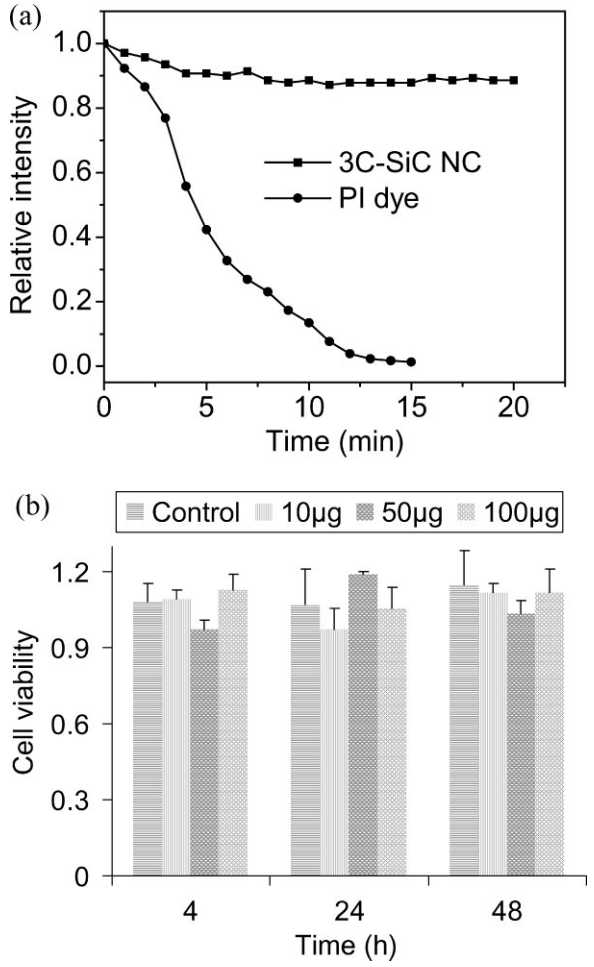

Figure 6. a) Photostability tests on 3C–SiC nanocrystal-labeled and PI-dye-labeled hFOB cells excited at 420–490 nm and at 545 nm, respectively. b) Cytotoxicity evaluation. HeLa cells were incubated with different concentrations of 3C–SiC nanocrystals as indicated for 4, 24, and 48 h, and then analyzed by the standard MTT assay (see Experimental Section). Error bars indicate the standard deviation for three independent experiments.

visible spectral range with photon energies higher than ≈2.2 eV. By improving the size monodispersity of the nanoparticles with methods such as size-selective precipitation, the nanoparticles are expected to have wider use in multicolor imaging in various biological systems.

Experimental Section

Fabrication and characterization of 3C–SiC nanocrystals: The details of the procedure to synthesize 3C–SiC nanocrystals can be found in our previous report.[21] Note that the etching current density used here was 30 mA cm^{-2}. The infrared transmission spectra were acquired on a PerkinElmer 100 FT-IR spectrometer. The UV/Vis absorption spectra were obtained on an Agilent/HP-Germany 8453 UV/Vis spectrophotometer. The fluorescence spectral analysis was conducted on a Fluorolog-TCSPC spectrofluorometer with the Xe lamp and pulsed-laser diodes as the excitation sources. The fluorescence microscopy analysis for bioimaging was performed on a ZEISS Axioplan 2 fluorescence microscope using continuous-wave excitation provided by a 100 W HBO 103 mercury vapor lamp. The images were captured with a cooled CCD camera connected to a computer with AxioVision software.

Nanocrystal uptake: hFOB cells were cultured in a complete medium made of a mixture of 45% Dulbecco's modified eagle medium (DMEM; Invitrogen Cat no. 11995-040), 45% F-12 (Invitrogen Cat no. 11765-047), and 10% fetal calf serum (FCS, Hyclone Cat no. SV30087.02). The culture was maintained at 37 °C under 95% air and 5% CO_2. Suspensions of 3C–SiC nanocrystals (1 mg mL^{-1}) were prepared with phosphate buffered saline (PBS). After ultrasonic treatment for 10 min to ensure complete dispersion of the nanocrystals, a 0.5 mL suspension was added into a 60-mm dish containing the cells that had been plated 24 h before. The dish was then incubated at 37 °C in a CO_2 incubator for 2 h for nanocrystal uptake. Afterwards, the samples were rinsed with PBS four times to remove the excess nanocrystals and then fixed with 2% paraformaldehyde before microscopy measurements. The cells in the reference sample were stained with PI by using a similar procedure.

Cytotoxicity test: Human cervical carcinoma cells HeLa were purchased from ATCC (ATCC number CCL2) and maintained at 37 °C and in 5% CO_2, in DMEM, supplemented with 10% fetal bovine serum and 1% penicillin/streptomycin. 24 h before the experiment, equal amounts of HeLa cells were seeded in three rows of wells of a 96-well plate so that the cell confluence in all wells at the start of the experiment was 25%. On the day of the experiment, the first row of wells was treated with the 3C–SiC nanocrystals at different final concentrations (0, 10, 50, or 100 μg mL^{-1} diluted with culture medium; three wells for each concentration). Other wells were unperturbed. The plate was then returned to the incubator. 24 h later, the second row of wells was treated with various concentrations of the nanocrystals, as above. After another 20 h, the third row was treated similarly. 4 h later, all the wells were washed with a fresh medium and 200 μL of the fresh medium was added to each well. In effect, the cells in the first row of the wells had been incubated in the various concentrations of the nanocrystals for 48 h, the cells in the second row for 24 h, and the cells in the third row for 4 h. A 20 μL aliquot of the MTT working solution (0.1 g MTT powder in 20 mL PBS) was then added into each well and the plate was incubated at 37 °C for 1 h, after which 100 μL of the stopping solution (10 g sodium dodecyl sulfate in 50 mL isobutanol and 50 mL 0.01 N HCl) was added into each well to stop the reaction and dissolve the newly formed MTT formazan crystals. MTT reduction activity was examined by measuring the absorbance of the extracted solution at 600 nm using UV/Vis spectrophotometry (SpectraMAX 340, Molecular Devices).

Keywords:

biological labeling · fluorescence · nanoparticles · silicon carbide

[1] X. Michalet, F. F. Pinaud, L. A. Bentolila, J. M. Tsay, S. Doose, J. J. Li, G. Sundaresan, A. M. Wu, S. S. Gambhir, S. Weiss, *Science* **2005**, *307*, 538–544.

[2] S. M. Nie, Y. Xing, G. J. Kim, J. W. Simons, *Annu. Rev. Biomed. Eng.* **2007**, *9*, 257–288.

[3] A. M. Derfus, W. C. W. Chan, S. N. Bhatia, *Nano Lett.* **2004**, *4*, 11–18.
[4] C. Kirchner, T. Liedl, S. Kudera, T. Pellegrino, A. M. Javier, H. E. Gaub, S. Stölzle, N. Fertig, W. J. Parak, *Nano Lett.* **2005**, *5*, 331–338.
[5] Z. F. Li, E. Ruckenstein, *Nano Lett.* **2004**, *4*, 1463–1467.
[6] S. J. Yu, M. W. Kang, H. C. Chang, K. M. Chen, Y. C. Yu, *J. Am. Chem. Soc.* **2005**, *127*, 17604–17605.
[7] C. C. Fu, H. Y. Lee, K. Chen, T. S. Lim, H. Y. Wu, P. K. Lin, P. K. Wei, P. H. Tsao, H. C. Chang, W. Fann, *Proc. Natl. Acad. Sci. USA* **2007**, *104*, 727–732.
[8] L. Cao, X. Wang, M. J. Meziani, F. Lu, H. Wang, P. G. Luo, Y. Lin, B. A. Harruff, L. M. Veca, D. Murray, S. Y. Xie, Y. P. Sun, *J. Am. Chem. Soc.* **2007**, *129*, 11318–11319.
[9] P. Mélinon, B. Masenelli, F. Tournus, A. Perez, *Nat. Mater.* **2007**, *6*, 479–490.
[10] T. Matsumoto, J. Takahashi, T. Tamaki, T. Futagi, H. Mimura, Y. Kanemitsu, *Appl. Phys. Lett.* **1994**, *64*, 226–228.
[11] J. S. Shor, L. Bemis, A. D. Kurtz, I. Grimberg, B. Z. Weiss, M. F. MacMillian, W. J. Choyke, *J. Appl. Phys.* **1994**, *76*, 4045–4049.
[12] A. O. Konstantinov, A. Henry, C. I. Harris, E. Janzén, *Appl. Phys. Lett.* **1995**, *66*, 2250–2252.
[13] V. Petrova-Koch, O. Sreseli, G. Polisski, D. Kovalev, T. Muschik, F. Koch, *Thin Solid Films* **1995**, *255*, 107–110.
[14] L. S. Liao, X. M. Bao, Z. F. Yang, N. B. Min, *Appl. Phys. Lett.* **1995**, *66*, 2382–2384.
[15] T. L. Rittenhouse, P. W. Bohna, T. K. Hossain, I. Adesida, J. Lindesay, A. Marcus, *J. Appl. Phys.* **2004**, *95*, 490–496.
[16] J. Y. Fan, X. L. Wu, P. K. Chu, *Prog. Mater. Sci.* **2006**, *51*, 983–1031. and references therein.
[17] A. Kassiba, M. Makowska-Janusik, J. Bouclé, J. F. Bardeau, A. Bulou, N. Herlin-Boime, *Phys. Rev. B* **2002**, *66*, 155317.
[18] J. Bouclé, N. Herlin-Boime, A. Kassiba, *J. Nanopart. Res.* **2005**, *7*, 275–285.
[19] J. Bouclé, A. Kassiba, M. Makowska-Janusik, N. Herlin-Boime, C. Reynaud, A. Desert, J. Emery, A. Bulou, J. Sanetra, A. A. Pud, S. Kodjikian, *Phys. Rev. B* **2006**, *74*, 205417.
[20] X. L. Wu, J. Y. Fan, T. Qiu, X. Yang, G. G. Siu, P. K. Chu, *Phys. Rev. Lett.* **2005**, *94*, 026102.
[21] J. Y. Fan, X. L. Wu, H. X. Li, H. W. Liu, G. G. Siu, P. K. Chu, *Appl. Phys. Lett.* **2006**, *88*(04), **1909.**
[22] J. Botsoa, J. M. Bluet, V. Lysenko, O. Marty, D. Barbier, G. Guillot, *J. Appl. Phys.* **2007**, *102*, 083526.
[23] S. H. Tolbert, A. B. Herhold, C. S. Johnson, A. P. Alivisatos, *Phys. Rev. Lett.* **1994**, *73*, 3266–3269.
[24] J. N. Demasa, G. A. Crosby, *J. Phys. Chem.* **1971**, *75*, 991–1024.
[25] W. L. Wilson, P. F. Szajowski, L. E. Brus, *Science* **1993**, *262*, 1242–1244.
[26] M. Bruchez, Jr., M. Moronne, P. Gin, S. Weiss, A. P. Alivisatos, *Science* **1993**, *281*, 2013–2016.
[27] L. E. Brus, P. F. Szajowski, W. L. Wilson, T. D. Harris, S. Schuppler, P. H. Citrin, *J. Am. Chem. Soc.* **1995**, *117*, 2915–2922.
[28] F. A. Reboredo, L. Pizzagalli, G. Galli, *Nano Lett.* **2004**, *4*, 801–804.
[29] X.-H. Peng, S. K. Nayak, A. Alizadeh, K. K. Varanasi, N. Bhate, L. B. Rowland, S. K. Kumar, *J. Appl. Phys.* **2007**, *102*, 024304.
[30] *The Sadtler Handbook of Infrared Spectra* (Ed.: W. H. Simons), Sadtler Research Laboratories, Philadelphia **1978**.
[31] H. Richter, Z. P. Wang, L. Ley, *Solid State Commun.* **1981**, *39*, 625–629.
[32] F. Amy, Y. J. Chabal, *J. Chem. Phys.* **2003**, *119*, 6201–6209.
[33] G. Cicero, A. Catellani, G. Galli, *Phys. Rev. Lett.* **2004**, *93*, 016102.
[34] G. Cicero, J. C. Grossman, A. Catellani, G. Galli, *J. Am. Chem. Soc.* **2005**, *127*, 6830–6835.
[35] J. Jiang, K. F. Huo, Z. W. Wu, S. H. Chen, S. H. Pu, Z. L. Yu, X. Y. Liu, P. K. Chu, *Biomaterials* **2008**, *29*, 544–550.
[36] S. D. Conner, S. L. Schmid, *Nature* **2003**, *422*, 37–42.
[37] A. M. Schrand, H. Huang, C. Carlson, J. J. Schlager, E. Ōsawa, S. M. Hussain, L. Dai, *J. Phys. Chem. B* **2007**, *111*, 2–7.
[38] Y. Kanai, G. Cicero, A. Selloni, R. Car, G. Galli, *J. Phys. Chem. B* **2005**, *109*, 13656–13662.

Received: January 16, 2008
Revised: April 6, 2008
Published online: July 10, 2008

